A Definitive Investigation of the Gas-Phase Two-Center Three-Electron Bond in $[H_2S\therefore SH_2]^+$, $[Me_2S\therefore SMe_2]^+$, and $[Et_2S\therefore SEt_2]^+$: Theory and Experiment

Ying Deng, Andreas J. Illies,* Mary A. James, Michael L. McKee,* and Michael Peschke†

Contribution from Department of Chemistry, Auburn University, Auburn, Alabama 36849-5312

Received March 8, 1994⊗

Abstract: The association products of reactions 1 and 2, examples of two-center three-electron (2c-3e) S∴S bonds, were studied in the gas phase. $Me_2S^+ + SMe_2 + M \rightleftarrows [Me_2S\therefore SMe_2]^+ + M$ (1) and $Et_2S^+ + SEt_2 + M \rightleftarrows [Et_2S\therefore SEt_2]^+ + M$ (2). The binding enthalpies were determined by measuring the temperature dependence of the equilibrium constants for eqs 1 and 2. The experimental bond enthalpy and entropy of association were determined for reaction 1 at 576 K ($\Delta H^\circ_{bond,576} = 111 \pm 2$ kJ/mol, $\Delta S^\circ_{rxn,576} = -112 \pm 3$ J/mol K) and for reaction 2 at 520 K ($\Delta H^\circ_{bond,520} = 116 \pm 3$ kJ/mol, $\Delta S^\circ_{rxn,520} = -132 \pm 5$ J/mol K). The calculated bond enthalpies with zero-point and heat capacity corrections are 122 kJ/mol at 576 K at the [PMP4/6-31+G(2df,p)]//MP2/6-31G(d) level and 112 kJ/mol for $[Et_2S\therefore SEt_2]^+$ at 520 K at the PMP2/6-31G(d)//HF/6-31G(d) level. Three conformations of Et_2S and Et_2S^+ are predicted to be within 4 kJ/mol of each other. The preferred $[Et_2S\therefore SEt_2]^+$ 2c-3e complex (C_2 symmetry) is formed between C_1 conformers of Et_2S and Et_2S^+. The calculated bond energy for $[H_2S\therefore SH_2]^+$ is 119.6 kJ/mol using G2 theory. All three 2c-3e complexes were further studied by calculating the lowest optical transition and the hydrogen hyperfine coupling constants.

I. Introduction

The sulfur−sulfur bonds in $[H_2S\therefore SH_2]^+$, $[Me_2S\therefore SMe_2]^+$ ($(DMS)_2^+$), and $[Et_2S\therefore SEt_2]^+$ ($(DES)_2+$) are examples of two-center three-electron (2c-3e) bonds[1,2] which were first described in 1931 by Linus Pauling.[3] A simple molecular orbital representation of this form of bonding is shown by the potential energy diagram.

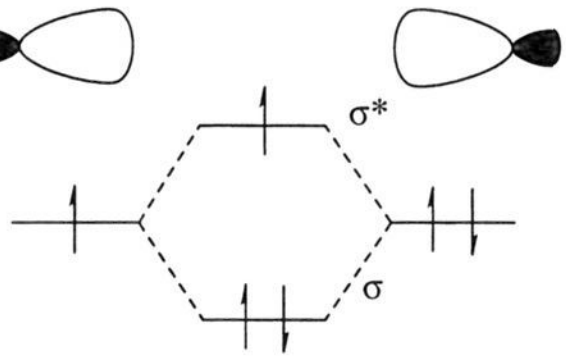

Despite the interest in S∴S 2c-3e bonds,[4−23] very few experiments have directly probed the nature of these bonds. The complexes are easily formed in solution and give rise to distinctive ESR[24] and visible[25] spectra from which indirect information on the nature of the 2c-3e S∴S bond can be obtained.[26] On the other hand, 2c-3e bonds have been the subject of numerous theoretical investigations.[27−32] Our interest is to directly determine the gas-phase bond energy. Our earlier efforts[33] were hampered by a small temperature range in the mass spectral study. It was possible to place limits on the bond energy, but a definitive measurement was not possible.

† Authors appear in alphabetical order.

⊗ Abstract published in *Advance ACS Abstracts,* November 15, 1994.

(1) Baird, N. C. *J. Chem. Ed.* **1977**, *54*, 291.
(2) Harcourt, R. D. *J. Chem. Ed.* **1985**, *62*, 99.
(3) Pauling, L. *J. Am. Chem. Soc.* **1931**, *53*, 3225.
(4) Hungerbühler, H.; Guha, S. N.; Asmus, K.-D. *J. Chem. Soc., Chem. Commun.* **1991**, 999.
(5) Bobrowski, K.; Schöneich, C.; Holcman, J.; Asmus, K.-D. *J. Chem. Soc., Perkin Trans. 2* **1991**, 353.
(6) Anklam, E.; Asmus, K.-D.; Mohan, H. *J. Phys. Org. Chem.* **1990**, *3*, 17.
(7) Kishore, K.; Asmus, K.-D. *J. Chem. Soc., Perkin Trans. 2* **1989**, 2079.
(8) Drewello, T.; Lebrilla, C. B.; Asmus, K.-D.; Schwarz, H. *Angew. Chem., Int. Ed. Engl.* **1989**, *28*, 1275.
(9) Anklam, E.; Mohan, H.; Asmus, K.-D. *J. Chem. Soc., Perkin Trans. 2* **1988**, 1297.
(10) Mohan, H.; Asmus, K.-D. *J. Phys. Chem.* **1988**, *92*, 118.
(11) Anklam, E.; Mohan, H.; Asmus, K.-D. *J. Chem. Soc., Chem. Commun.* **1987**, 629.
(12) Drewello, T.; Lebrilla, C. B.; Schwarz, H.; de Koning, L. J.; Fokkens, R. H.; Nibbering, N. M. M.; Anklam, E.; Asmus, K.-D. *J. Chem. Soc., Chem. Commun.* **1987**, 1381.
(13) Mönig, J.; Goslich, R.; Asmus, K.-D. *Ber. Bunsen-Ges. Phys. Chem.* **1986**, *90*, 115.
(14) Bonifačić, M.; Asmus, K.-D. *J. Org. Chem.* **1986**, *51*, 1216.
(15) Bonifačić, M.; Weiss, J.; Chaudhri, S. A.; Asmus, K.-D. *J. Phys. Chem.* **1985**, *89*, 3910.
(16) Mönig, J.; Göbl, M.; Asmus, K.-D. *J. Chem. Soc., Perkin Trans. 2* **1985**, 647.
(17) Göbl, M.; Bonifačić, M.; Asmus, K.-D. *J. Am. Chem. Soc.* **1984**, *106*, 5984.
(18) Chaudhri, S. A.; Göbl, M.; Freyholdt, T.; Asmus, K.-D. *J. Am. Chem. Soc.* **1984**, *106*, 5988.
(19) Bahnemann, D.; Asmus, K.-D.; Willson, R. L. *J. Chem. Soc., Perkin Trans. 2* **1981**, 890.
(20) Asmus, K.-D.; Bahnemann, D.; Fischer, Ch.-H.; Veltwisch, D. *J. Am. Chem. Soc.* **1979**, *101*, 5322.
(21) Asmus, K.-D. *Acc. Chem. Res.* **1979**, *12*, 436.
(22) Syage, J. A.; Pollard, J. E.; Cohen, R. B. *J. Phys. Chem.* **1991**, *95*, 8560.
(23) Belloni, J.; Marignier, J. L.; Katsumura, Y.; Tabata, Y. *J. Phys. Chem.* **1986**, *90*, 4014.
(24) Gilbert, B. C. In *Sulfur-Centered Reactive Intermediates in Chemistry and Biology*; Chatgilialoglu, C., Asmus, K.-D., Eds.; Plenum Press: New York, 1990; p 135.
(25) Asmus, K.-D. In *Sulfur-Centered Reactive Intermediates in Chemistry and Biology*; Chatgilialoglu, C., Asmus, K.-D., Eds.; Plenum Press: New York, 1990; p 155.
(26) Bally, T. In *Radical Ionic Systems*; Lund, A., Shiotani, M., Eds.; Kluwer Academic Publishers: The Netherlands, 1991; pp 3−54.
(27) Clark, T. *J. Am. Chem. Soc.* **1988**, *110*, 1672.
(28) Clark, T. *J. Comput. Chem.* **1983**, *4*, 404.
(29) Clark, T. *J. Comput. Chem.* **1982**, *3*, 112.
(30) Clark, T. *J. Comput. Chem.* **1981**, *2*, 261.
(31) Gill, P. M. W.; Weatherall, P.; Radom, L. *J. Am. Chem. Soc.* **1989**, *111*, 2782.
(32) Gill, P. M. W.; Radom, L. *J. Am. Chem. Soc.* **1988**, *110*, 4931.

0002-7863/95/1517-0420$09.00/0 © 1995 American Chemical Society

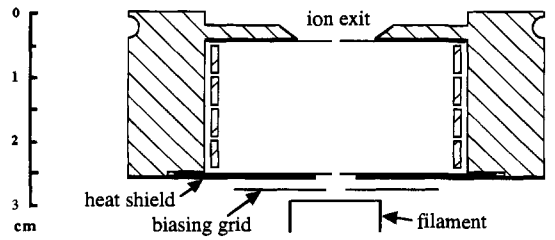

Figure 1. Schematic cross-section of the new ion source showing internal drift guard rings. The electron entrance plate is electrically insulated from the source block and heat shield by mica gaskets. The drift length is 2.0 cm, while the inside drift guard diameter is 3.0 cm.

In the present paper, we present a more thorough study of the measured and theoretically predicted sulfur−sulfur interactions in $[Me_2S\therefore SMe_2]^+$ and $[Et_2S\therefore SEt_2]^+$. $[H_2S\therefore SH_2]^+$ was only theoretically studied, since the proton-bound dimer rather than the 2c-3e complex is formed in the gas phase at high ion source pressures. The experimental goals of our studies are to determine $\Delta G°_{rxn}$ from equilibrium studies and the bond enthalpy ($\Delta H°_{bond}$) from the temperature dependence. Theoretically, the goals include calculating the bond energy, entropy of association, geometry, electron densities, λ_{max}, and hyperfine coupling constants.

The previously reported experimental estimate of the bond enthalpy for $[Me_2S\therefore SMe_2]^+$ was derived from high-pressure mass spectrometric studies of the equilibrium constant for reaction 1 at a single temperature (hence a single determination of $\Delta H°_{rxn}$ combined with an estimate of the entropy of reaction).[33] Due to the relatively strong S∴S bond, high temperatures were required for the equilibrium study, and we were only able to make measurements at the high-temperature limit of our apparatus. Thus, the experimental bond enthalpy estimate for the 2c-3e interaction in $[Me_2S\therefore SMe_2]^+$ was in the range 100−111 kJ/mol. Ab initio calculations at the [PMP2/6-31G(d)]//3-21G(d) level gave a bond energy of 109.6 kJ/mol[33] (the brackets indicate that the additivity approximation[34] was used).

In earlier experiments, the enthalpy of reaction for the iodine−iodine interaction in $[CH_3I\therefore ICH_3]^+$ was estimated to be in the range −96 to −109 kJ/mol.[35,36] This range represents about 65% of the iodine−iodine interaction in I_2[37] and is in excellent agreement with the result reported for the iodine−iodine 2c-3e bonding interaction of 102 kJ/mol in I_2^-.[27] We believe that these studies on $[Me_2S\therefore SMe_2]^+$ and $[CH_3I\therefore ICH_3]^+$ represented the first gas-phase experimental binding results for well-characterized 2c-3e bonds between heteroatoms in organic molecules. The present study offers more detailed experimental bond information as well as new theoretical insights into this type of bonding.

II. Experimental Section

A redesigned ion source (Figure 1) capable of a much larger temperature range (90−650 K) and improved thermalization of all source parts was used in the present studies. The source has been described elsewhere in detail.[38] Of importance here is the fact that the ion exit aperture is mounted **inside** a large copper block. This ensures that the entire region near the ion exit is at the same temperature as the source block itself. The electron filament was shielded first by a biasing plate and second by a thermal shield, thus reducing the "hot spot" near the ionizing filament. As in previous designs, internal drift guard rings shaped and controlled the electric fields (Figure 1).[38−40]

It should be noted that the ionization voltage was very low (9−15 V) which means the electrons do not penetrate far into the ion source but rather form ions only near the electron entrance hole. All of the charges were pulled through the entire length of the ion source by the extraction voltage and underwent many thousands of collisions during the transit time of >100 μs.[41] Hence, the ions were well thermalized with little initial excess energy, resulting in reduced fragmentation and therefore simple high-pressure mass spectra.[38−42]

Our arrangement may be contrasted to high-pressure ion sources that use conventional 90° electron entrance−ion exit geometry. At voltages typical for these geometries (>1000 V), electrons produce an electrical plasma and are scattered throughout the source, including the region near the ion exit slit, where they cause ionization.[43] Residence time distributions (RTD's) for these sources, therefore, usually show reactant ion signals near $t = 0$.[44] These ions have not undergone many switching reactions and are not in equilibrium. Hence, RTD's from these sources do not achieve constant product-to-reactant ion ratios (and equilibria) until some time after the ionizing pulse.[43−45]

An earlier published study[46] on the bonding in $H_3O^+CO_2$ and $H_3O^+N_2O$ showed that our new source gave results that compare very well with results from other groups using different ion source configurations. In the case of $H_3O^+CO_2$, other groups obtained bond enthalpies that ranged from 59.8 to 64.0 kJ/mol and entropies of association that ranged from −86.6 to −102.9 J/mol K.[47] With our source we obtained an experimental bond enthalpy of 56.1 kJ/mol and an entropy of association of −82.8 J/mol K, which agrees very well with a high level ab initio study.[48] In the case of $H_3O^+N_2O$, the result from unpublished work by Szulejko and McMahon was 66.1 kJ/mol for the experimental bond enthalpy and −93.7 J/mol K for the entropy of association.[47a] Our experimental bond enthalpy was 65.3 kJ/mol, and the entropy of association was −100.8 J/mol K,[46] which again agrees very well with a published ab initio study.[49]

In the present studies on $[Me_2S\therefore SMe_2]^+$, total ion source pressures ranged from 0.50 to 0.73 Torr. The Me_2S (DMS) concentration covered the range 5.9−14.8 mol% in CF_4 bath gas. The $[Et_2S\therefore SEt_2]^+$ experiments were carried out in CF_4 bath gas with total ion source pressures ranging from 0.31 to 0.45 Torr and the Et_2S (DES) concentration ranging from 1.9 to 4.7 mol%. The reactant gas, Me_2S

(33) Illies, A. J.; Livant, P.; McKee, M. L. *J. Am. Chem. Soc.* **1988**, *110*, 7980.
(34) (a) McKee, M. L.; Lipscomb, W. N. *J. Am. Chem. Soc.* **1981**, *103*, 4673. (b) Nobes, R. H.; Bouma, W. J.; Radom, L. *Chem. Phys. Lett.* **1982**, *89*, 497. (c) McKee, M. L.; Lipscomb, W. N. *Inorg. Chem.* **1985**, *24*, 762.
(35) Livant, P.; Illies, A. *J. Am. Chem. Soc.* **1991**, *113*, 1510.
(36) (a) The association energy of $[CH_3I\therefore ICH_3]^+$ was calculated[36b] to be −85.8 kJ/mol and the I−I distance was calculated to be 3.419 Å at the PMP4/LANL1DZ//UHF/LANL1DZ level.[36c] (b) McKee, M. L. Unpublished results. (c) Hay, P. J.; Wadt, W. P. *J. Chem. Phys.* **1985**, *82*, 270. Wadt, W. R.; Hay, P. J. *J. Chem. Phys.* **1985**, *82*, 284. Hay, P. J.; Wadt, W. R. *J. Chem. Phys.* **1985**, *82*, 299.
(37) Chase, M. W., Jr.; Davies, C. A.; Downey, J. R., Jr.; Frurip, D. J.; McDonald, R. A.; Syverud, A. N. *J. Phys. Chem. Ref. Data* **1985**, *14* (Suppl. 1), 1.
(38) Illies, A. J. *Org. Mass Spectrom.* **1990**, *25*, 73.
(39) Illies, A. J. *J. Phys. Chem.* **1988**, *92*, 2889.
(40) van Koppen, P. A. M.; Kemper, P. R.; Illies, A. J.; Bowers, M. T. *Int. J. Mass Spectrom. Ion Processes* **1983**, *54*, 263.
(41) Illies, A. J. *Org. Mass Spectrom.* **1989**, *24*, 186.
(42) (a) Meisels, G. G.; Illies, A. J. *Anal. Chem.* **1981**, *53*, 2162. (b) Polley, C. W.; Illies, A. J.; Meisels, G. G. *Anal. Chem.* **1980**, *52*, 1797. (c) Illies, A. J.; Meisels, G. G. *Anal. Chem.* **1980**, *52*, 325. (d) Kemper, P. R.; Bowers, M. T. *J. Am. Soc. Mass Spectrom.* **1990**, *1*, 197.
(43) Kebarle, P. In *Techniques for the Study of Ion-Molecule Reactions*; Farrar, J. M., Saunders, W. H., Jr., Eds.; Wiley and Sons, Inc.: New York, 1988; pp 221−286.
(44) Durden, D. A.; Kebarle, P.; Good, A. *J. Chem. Phys.* **1969**, *50*, 805.
(45) (a) Good, A.; Durden, D. A.; Kebarle, P. *J. Chem. Phys.* **1970**, *52*, 222. (b) Good, A.; Durden, D. A.; Kebarle, P. *J. Chem. Phys.* **1970**, *52*, 212.
(46) Ekern, S. P.; Deng, Y.; Snowden, K. J.; McKee, M. L.; Illies, A. *J. Phys. Chem.* **1992**, *96*, 10176.
(47) (a) Szulejko, J. E.; McMahon, T. B. Unpublished work. (b) Hiraoka, K.; Shoda, T.; Morise, K. *J. Chem. Phys.* **1986**, *84*, 2091. (c) Meot-Ner, M.; Field, F. H. *J. Chem. Phys.* **1977**, *66*, 4527.
(48) The ab initio value for $H_3O^+CO_2$ at the [QCISD(T)/6-31+G(2d,p)]//MP2/6-31G(d) level is 55.6 kJ/mol for the bond enthalpy and −89.1 J/mol K for the entropy of association. The brackets indicate that the additivity approximation has been used (ΔE(QCISD(T)/6-31+G(2d,p)) = ΔE(QCISD(T)/6-31G(D)) + ΔE(MP4/6-31+G(2d,p)) − ΔE(MP4/6-31G(d)).[46]
(49) The ab initio value for H_3O^+ONN at the [QCISD(T)/6-31+G(2d,p)]//MP2/6-31G(d) level is 58.6 kJ/mol for the bond enthalpy and −98.7 J/mol K for the entropy of association.[46] For brackets, see ref 48.

Table 1. Total Energies (hartrees) and Zero-Point Energies (kJ/mol) for Various Species[a]

			//HF/6-31G(d)[b]			//MP2/6-31G(d)				
	sym	sta	HF/a	PMP2/a	ZPE[c]/a	MP2/a	PMP2/a	PMP4/a	PMP2/b	G2[d]
SH_2 **1**	C_{2v}	$^1A_1$	−398.66732	−398.78821	43.2 (0)	−398.78841	−398.78841	−398.81200	−398.85551	−398.93072
SH_2^+ **1**$^+$	C_{2v}	$^2B_1$	−398.32699	−398.42719	42.6 (0)	−398.42562	−398.42751	−398.45100	−398.48129	−398.54744
$(SH_2)_2^+$	C_{2h}	^2B_u	−797.02610	−797.26395	100.2 (0)	−797.26162	−797.26461	−797.31048	−797.38999	−797.52371
$H_2S{\cdot}2H_2O$	C_s	$^1A'$	−550.69777[e]	−551.19153[e]	172.9 (0)[e]	−551.20092	−551.20092	−551.24460	−551.42976	
$H_2S{\cdot}2H_2O^+$	C_s	$^2A''$	−550.41162	−550.89446	178.3 (1)	−550.89288	−550.89468	−550.93621	−551.10483	
$H_4S_2{\cdot}4H_2O^+$	C_i	^2A_u	−1101.14725	−1102.13918	367.1 (0)	−1102.14204	−1102.14488	−1102.22892	−1102.59006	
DMS **2**	C_{2v}	$^1A_1$	−476.73533	−477.12066	214.1 (0)	−477.12111	−477.12111	−477.17503	−477.26052	
DMS$^+$ **2**$^+$	C_{2v}	$^2B_1$	−476.45471	−476.81704	211.6 (0)	−476.81573	−476.81776	−476.87232	−476.94651	
$(DMS)_2^+$	C_{2h}	^2B_u	−953.21557	−953.98535	433.1 (0)	−953.98357	−953.98657	−954.09277	−954.26001	
DES **3a**	C_{2v}	$^1A_1$	−554.80562	−555.45409	375.4 (0)					
DES **3b**	C_2	^1A	−554.80429	−555.45400	375.4 (0)					
DES **3c**	C_s	$^1A'$	−554.80253	−555.45201	374.9 (1)					
DES **3d**	C_1	^1A	−554.80496	−555.45402	375.4 (0)					
DES$^+$ **3a**$^+$	C_{2v}	$^2B_1$	−554.53569	−555.15955	372.6 (0)					
DES$^+$ **3b**$^+$	C_2	^2B	−554.53390	−555.15908	375.4 (0)					
DES$^+$ **3c**$^+$	C_s	$^2A'$	−554.53247	−555.15731	374.1 (1)					
DES$^+$ **3d**$^+$	C_1	^2A	−554.53475	−555.15928	373.5 (0)					
$(DES)_2^+$	C_{2h}	^2B_u	−1109.35868	−1110.65790	754.8 (3)					
$(DES)_2^+$	C_2	^2B	−1109.36159	−1110.66046	754.6 (0)					

[a] Basis set a is 6-31G(d). Basis set b is 6-31+G(2df,p). [b] Spin-squared value for open-shell species were between 0.76 and 0.78. [c] Zero-point energy (kJ/mol) with number of imaginary frequencies in parentheses. [d] G2 method, ref 54. [e] The HF/6-31G(d) geometry is assumed to be SH_2 plus $(H_2O)_2$.

or Et_2S, was mixed with the bath gas in the ion source inlet system by introducing the gases through separate leak valves. Gas pressures were measured with an MKS capacitance manometer. Mass spectra were recorded using conventional analog recording techniques, while residence time distributions and ion intensity measurements for the determination of equilibrium constants were collected using previously described pulse-counting techniques.[39,40]

Computational Methods. After comparison of MNDO,[50a] AM1,[50b] and PM3[50c] with ab initio results on the thiirane 2c-3e complex in a previous publication,[51] MNDO was chosen in the present study to survey the Et_2S and $[Et_2S\therefore SEt_2]^+$ stationary points. The MNDO geometries were used as starting positions of ab initio optimizations using the Gaussian92 program system.[52] All geometries were optimized at the HF/6-31G(d) level, and frequencies were calculated at that level to confirm the nature of the stationary point and to make corrections for zero-point energies (0.9 weighting factor). Single-point calculations were made at the PMP2/6-31G(d) level where "P" indicates that the effect of spin contamination has been projected out of the MP energy.[53] Additional optimizations at the MP2/6-31G(d) level were carried out for all species except Et_2S, Et_2S^+, and $[Et_2S\therefore SEt_2]^+$. At MP2/6-31G(d) geometries, single-point calculations were made at the PMP4/6-31G(d) and PMP2/6-31+G(2df,p) levels and combined using the additivity approximation[34] to estimate relative energies at the [PMP4/6-31+G(2df,p)] level. For H_2S, H_2S^+, and $[H_2S\therefore SH_2]^+$, G2 theory, which estimates energies at the [QCISD(T)/6-311+G(3df,2p)] level with corrections for zero-point energy and higher order effects, was applied. G2 theory[54] has been shown to yield results of chemical accuracy and has been applied to several studies of sulfur-containing species.[55-57] The lowest excitation energy in the 2c-3e bonded species was calculated using CI singles method at the CIS/6-31G(d) level.[58] Thermodynamic corrections (to determine standard enthalpy, entropy, and free energy) were made using uncorrected vibrational frequencies at the HF/6-31G(d) level with standard methods[59] unless otherwise noted. Absolute and relative energies for all molecules and conformers are presented in Tables 1 and 2, respectively, while calculated geometries are given in Figure 2. Experimental microwave structures for SH_2, SH_2^+, and DMS are also included in Figure 2.[60]

Thermodynamic Equilibrium Measurements. The thermodynamic bond energies for $[Me_2S\therefore SMe_2]^+$ and $[Et_2S\therefore SEt_2]^+$ were determined from equilibrium measurements of the reversible reactions 1 and 2.

$$Me_2S^+ + SMe_2 + M \rightleftarrows [Me_2S\therefore SMe_2]^+ + M \quad (1)$$

$$Et_2S + SEt_2 + M \rightleftarrows [Et_2S\therefore SEt_2]^+ + M \quad (2)$$

Specifically, the van't Hoff equation (eq 3) yields the enthalpy and entropy of reaction.

$$\ln K_p = -\Delta H^\circ_{rxn}/RT + \Delta S^\circ_{rxn}/R \quad (3)$$

For association reactions, the enthalpy of reaction is the negative of the bond enthalpy. The bond energy (D°_o) is equal to the bond enthalpy at 0 K and can be related to the bond enthalpy at a different temperature by eq 4 where ΔC_p is the difference in heat capacities between reactants and products.

$$D^\circ_o = -\Delta H^\circ_{T,rxn} + \int_o^T \Delta C_p(T)\, dT \quad (4)$$

For ion−molecule association reactions, the heat capacity contribution of the cluster is usually larger due to a population of low-lying modes formed between the two reactant moieties; hence, the value for the bond energy is usually larger by about 4−8 kJ/mol than the value for the bond enthalpy. This difference is expected to be smaller the stronger the bond between the two moieties. Statistical thermodynamic heat capacity corrections for systems involving gas-phase ions are often

(50) (a) MNDO: Dewar, M. J. S.; Thiel, W. *J. Am. Chem. Soc.* **1977**, *99*, 4899, 4907. (b) AM1: Dewar, M. J. S.; Zoebisch, E. G.; Healy, E. F.; Stewart, J. J. P. *J. Am. Chem. Soc.* **1985**, *107*, 3902. (c) PM3: Stewart, J. J. P. *J. Comput. Chem.* **1989**, *10*, 209.

(51) Ekern, S.; Illies, A.; McKee, M. L.; Peschke, M. *J. Am. Chem. Soc.* **1993**, *115*, 12510.

(52) Frisch, M. J.; Trucks, G. W.; Head-Gordon, M.; Gill, P. M. W.; Wong, M. W.; Foresman, J. B.; Johnson, B. G.; Schlegel, H. B.; Robb, M. A.; Replogle, E. S.; Gomperts, R.; Andres, J. L.; Raghavachari, K.; Binkley, J. S.; Gonzalez, C.; Martin, R. L.; Fox, D. J.; DeFrees, D. J.; Baker, J.; Stewart, J. J. P.; Pople, J. A. *Gaussian92*; Gaussian, Inc.: Pittsburgh, PA, 1992.

(53) (a) Sosa, C.; Schlegel, H. B. *Int. J. Quantum Chem.* **1986**, *29*, 1001. (b) Schlegel, H. B. *J. Chem. Phys.* **1986**, *84*, 4530.

(54) Curtiss, L. A.; Raghavachari, K.; Trucks, G. W.; Pople, J. A. *J. Chem. Phys.* **1991**, *94*, 7221.

(55) Nobes, R. H.; Radom, L. *Chem. Phys. Lett.* **1992**, *189*, 554.

(56) Chiu, S. W.; Li, W.-K.; Tzeng, W.-B.; Ng, C.-Y. *J. Chem. Phys.* **1992**, *97*, 6557.

(57) Curtiss, L. A.; Nobes, R. H.; Pople, J. A.; Radom, L. *J. Chem. Phys.* **1992**, *97*, 6766.

(58) Foresman, J. B.; Head-Gordon, M.; Pople, J. A.; Frisch, M. J. *J. Phys. Chem.* **1992**, *96*, 135.

(59) McQuarrie, D. A. *Statistical Thermodynamics*; Harper & Row: New York, 1973.

(60) *Structure of Free Polyatomic Molecules*, Landolt-Börnstein, New Series; Madelung, O., Ed.; Springer-Verlag: New York, 1987; Vol. 15.

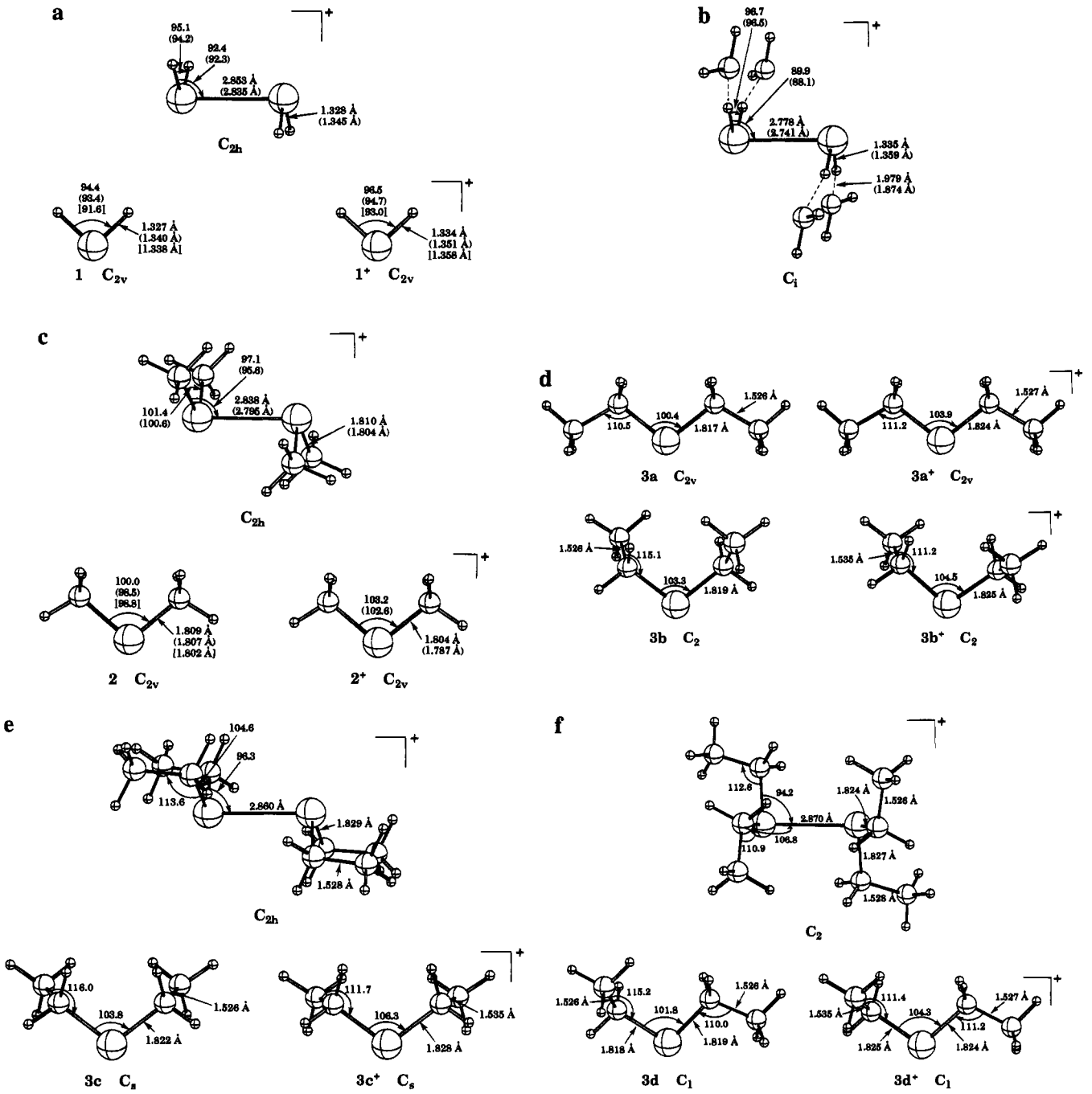

Figure 2. Calculated geometries for monomers and 2c-3e complexes at the HF/6-31G(d) level with MP2/6-31G(d) values in parentheses. Experimental microwave deterimations for SH_2, SH_2^+, and DMS given in brackets are from ref 60.

not possible since the vibrational frequencies and molecular geometries for ions are difficult to obtain. In the present study the parameters predicted by ab initio calculations are used to obtain the true bond energies.

In order to correctly determine experimental equilibrium constants, it must be demonstrated that the system is in true chemical equilibrium. We applied various tests to ensure that equilibrium exists. We measured RTD's for both reactant and product ions which indicate the time that the particular ions spend in the ion source. When a reaction is in chemical equilibrium, RTD's for reactant and product ions are identical because the charges undergo many switching reactions as they traverse the ion source, resulting in an averaging of the drift properties.[33,34,38,39] The RTD's were normalized by dividing each RTD by the maximum intensity (count). Overlapping RTD's clearly demonstrate that the product-to-reactant ion ratio is constant. Hence, if the RTD's are the same, it can be inferred that the system is at or near equilibrium. Apparent equilibrium constants were also measured as a function of composition, total ion source pressures, and ion extraction fields. The equilibrium data were extrapolated to zero extraction fields.

III. Results and Discussion

$[H_2S\therefore SH_2]^+$. There have been several previous theoretical calculations on the 2c-3e $[H_2S\therefore SH_2]^+$ complex.[27−32,61] Recent binding energies range from 111[31] to 124[27] kJ/mol while the S∴S distance is about 2.8 Å. Gill et al. have summarized the recent work.[32] Our G2 binding energy is 119.6 kJ/mol (Table 2) which is intermediate to the predictions at the PMP2/6-31G-(d)+ZPC and [PMP4/6-31+G(2df,p)]+ZPC levels, (114.5 and 123.5 kJ/mol, respectively, Table 2). The gas-phase S∴S

(61) (a) Fernández, P. F.; Ortiz, J. V.; Walters, E. A. *J. Chem. Phys.* **1986**, *84*, 1653. (b) Ortiz, J. V. *Chem. Phys. Lett.* **1987**, *134*, 366. (c) Kikuchi, O. *Bull. Chem. Soc. Jpn.* **1981**, *54*, 917.

Table 2. Relative Energies (kJ/mol) of Various Species[a]

	//HF/6-31G(d)			//MP2/6-31G(d)					
	HF/a	PMP2/a	+ZPC	PMP2/a	PMP4/a	PMP2/b	[PMP4/b][b]	+ZPC[c]	G2
SH_2 **1**	0.0	0.0	0.0	0.0	0.0	0.0	0.0	0.0	0.0
SH_2^+ $\mathbf{1}^+$	893.5	947.8	947.3	947.5	947.8	982.5	982.8	982.3	1006.3
$\mathbf{1} + \mathbf{1}^+$	0.0	0.0	0.0	0.0	0.0	0.0	0.0	0.0	0.0
$(SH_2)_2^+$	−83.4	−127.5	−114.5	−127.8	−124.7	−139.7	−136.6	−123.5	−119.6
$SH_2{\cdot}2H_2O$	0.0	0.0	0.0	0.0	0.0	0.0	0.0	0.0	0.0
$SH_2{\cdot}2H_2O^+$	751.3	779.9	784.8	804.0	809.6	853.1	858.7	863.6	
1(aq) + $\mathbf{1}^+$(aq)	0.0	0.0	0.0	0.0	0.0	0.0	0.0	0.0	
$(SH_2)_2^+$(aq)	−99.3	−139.7	−125.4	−129.4	−126.3	−145.6	−142.5	−128.2	
DMS **2**	0.0	0.0	0.0	0.0	0.0	0.0	0.0	0.0	
DMS$^+$ $\mathbf{2}^+$	736.8	797.2	795.0	796.4	794.7	824.4	822.7	820.5	
$\mathbf{2} + \mathbf{2}^+$	0.0	0.0	0.0	0.0	0.0	0.0	0.0	0.0	
$(DMS)_2^+$	−67.0	−125.1	−118.4	−125.2	−119.3	−139.0	−133.1	−126.4	
DES **3a**	0.0	0.0	0.0						
DES **3b**	1.9	0.2	0.2						
DES **3c**	8.1	5.4	5.0						
DES **3d**	1.8	0.2	0.2						
DES$^+$ $\mathbf{3a}^+$	708.7	773.4	770.9						
DES$^+$ $\mathbf{3b}^+$	713.4	774.5	774.5						
DES$^+$ $\mathbf{3c}^+$	717.1	779.2	778.0						
DES$^+$ $\mathbf{3d}^+$	711.2	774.0	772.3						
$\mathbf{3a} + \mathbf{3a}^+$	0.0	0.0	0.0						
$\mathbf{3b} + \mathbf{3b}^+$	8.2	1.5	4.0						
$\mathbf{3c} + \mathbf{3c}^+$	16.5	11.3	12.2						
$\mathbf{3d} + \mathbf{3d}^+$	4.2	0.8	1.6						
$(DES)_2^+(C_{2h})$	−45.6	−116.2	−110.1						
$(DES)_2^+(C_2)$	−53.2	−122.9	−117.0						

[a] Basis set a is 6-31G(d). Basis set b is 6-31+G(2df,p). [b] Additivity approximation is used. See ref 34. [c] Zero-point corrections are added to [PMP4/b] relative energies.

distance (2.835 Å) is identical to the value calculated by Gill et al.[32] at the same level (MP2/6-31G(d)). Since the only experimental observation of $[H_2S\therefore SH_2]^+$ has been in aqueous solution,[25] we also carried out calculations in which water molecules were allowed to interact explicitly with each hydrogen. At the MP2/6-31G(d) level, the oxygen−hydrogen distance is 1.626 Å in $H_2S^+{\cdot}2H_2O$ and 1.874 Å in $[H_2S\therefore SH_2]^+{\cdot}4H_2O$ (Figure 2), indicative of relatively strong hydrogen bonds. In contrast, in $H_2S{\cdot}2H_2O$, one H_2O is weakly hydrogen bonded to one hydrogen of H_2S (O···H 2.080 Å) while the second H_2O is hydrogen bonded to the first H_2O. This weak interaction between H_2S and water is in accord with its known limited solubility in water.[62] The S∴S bond energy remains almost unchanged on going from the gas phase to solution phase (i.e., $H_2S{\cdot}2H_2O + H_2S^+{\cdot}2H_2O \rightarrow [H_2S\therefore SH_2]^+{\cdot}4H_2O$) which suggests that the solvation energy of H_2S^+ and $[H_2S\therefore SH_2]^+$ are nearly the same. While the binding energy increases only 4.5 kJ/mol on going to the aqueous phase, the effect on the S∴S bond distance is more pronounced, shortening 0.094 Å. As will be discussed below, this difference will affect its visible spectrum. Schleyer and co-workers[63] found a similar shortening in the complex H_3BNH_3 (ΔBN = 0.05 Å at MP2/6-31G(d)) when they explicitly optimized the adduct with three waters around the nitrogen end. They suggested that the bond shortening was due to the dielectric reaction field of water (which would increase the dipole moment of H_3BNH_3). In the case of $[H_2S\therefore SH_2]^+{\cdot}4H_2O$, the explanation may be due to decreased electrostatic repulsion from a redistribution of positive charge to the solvent. At the UHF/6-31+G(2df,p) level, 0.14e$^-$ of charge has been transferred from the four solvent molecules to the 2c-3e cation.[64]

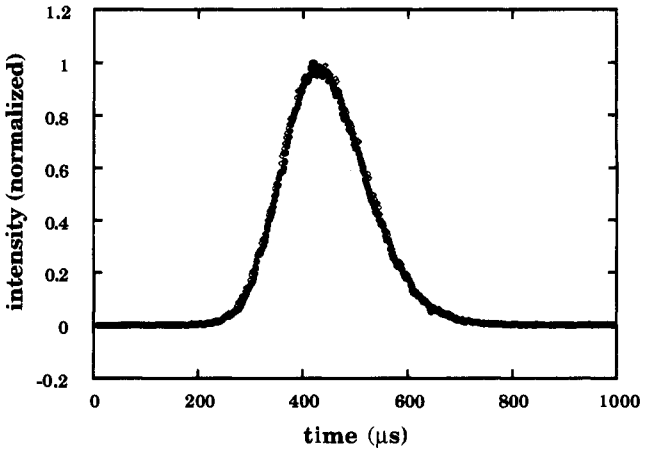

Figure 3. Normalized residence time distributions for Me_2S^+ (open diamonds) and $[Me_2S\therefore SMe_2]^+$ (filled circles) which indicate that the reactants and products in reaction 1 are at equilibrium.

$[Me_2S\therefore SMe_2]^+$. In an earlier paper the ion−molecule reactions responsible for the major peaks in the mass spectrum were identified.[33] Figure 3 shows that RTD's for Me_2S^+ and $[Me_2S\therefore SMe_2]^+$ collected with low drift potentials are identical. Measured apparent equilibrium constants, K_{app}, must also be invariant to the chemical composition (partial pressures). Experiments at various compositions and total ion source pressures were extrapolated to zero ion extraction volts at each temperature studied. At the lowest Me_2S^+ concentration, plots of K_{app} vs extraction voltage show a voltage dependence. At these low concentrations, equilibrium is not fully established, and the plots demonstrate kinetic approach to equilibrium as

(62) H_2S solubility: *CRC Handbook of Chemistry and Physics*, 71st ed.; Lide, D. R., Ed.; CRC Press: Boca Raton, FL, 1990−1991; pp 4−68.

(63) (a) Bühl, M.; Steinke, T.; Schleyer, P. v. R.; Boese, R. *Angew. Chem., Int. Ed. Engl.* **1991**, *30*, 1160. (b) More recently, see: Cremer, D.; Olson, L.; Reichel, F.; Kraka, E. *Isr. J. Chem.* **1993**, *33*, 369.

(64) A reviewer has suggested a plausible explanation for the S∴S bond shortening in solution. The lowest unoccupied orbital of the $[H_2S\therefore SH_2]^+$ complex (the S∴S σ^* orbital has one electron) involves a combination of the four S−H σ^* bonds with the right symmetry to overlap in a π fashion between the two sulfur atoms. The four explicit water molecules transfer charge into the LUMO which increases the S−H bond distances and decreases the S∴S distance.

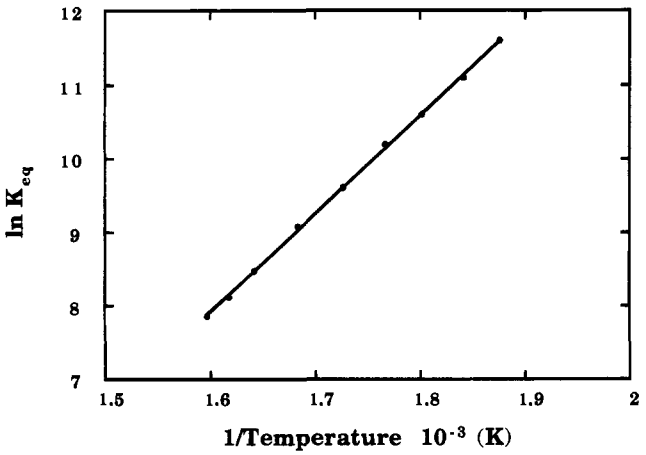

Figure 4. van't Hoff plot for reaction 1.

Table 3. Calculated Entropies (J/K mol) and Enthalpies (kJ/mol) of Association at Various Temperatures[a]

	298 K				520 K[b,c]		576 K[d]		
	ΔS	ΔH/a	ΔH/b	ΔH/c	ΔS	ΔH/a	ΔS	ΔH/a	ΔH/b
$(SH_2)_2^+$	−120[e]	−119	−128	−124					
$(DMS)_2^+$	−142[f]	−118	−126				−133	−114	−122
$(DES)_2^+$	−151	−116			−143	−112			

[a] Entropies are calculated at UHF/6-31G(d). Level a is PMP2/6-31G(d)//UHF/6-31G(d)+(0.9)ZPC/C_p//UHF/6-31G(d). Level b is [PMP4/6-31+G(2df,p)]//UMP2/6-31G(d)+(0.9)ZPC/C_p//UHF/6-31G(d). Level c is G2+C_p//UHF/6-31G(d). The symbol "(0.9)ZPC/C_p" indicates that the zero-point correction is made with a scaling factor of 0.9 and the heat capacity correction is made with unscaled frequencies. [b] The reference monomers for $(DES)_2^+$ are **3a**,**a**$^+$. If **3d**,**d**$^+$ are taken as the reference, the entropy and enthalpy of association become −150 J/K mol and −123 kJ/mol, respectively. [c] At 520 K the experimental entropy and enthalpy of association of $(DES)_2^+$ are −132 J/K mol and −116 kJ/mol, respectively. [d] At 576 K the experimental entropy and enthalpy of association of $(DMS)_2^+$ are −112 J/K mol and −111 kJ/mol, respectively. [e] The value of ΔS for $(SH_2)_2^+$ calculated at MP2/6-31G(d) is −120 J/K mol. [f] The value of ΔS for $(DMS)_2^+$ calculated at MP2/6-31G(d) is −143 J/K mol.

ion residence times increase with decreasing extraction voltage. As the Me_2S concentration is increased, the voltage dependence lessens and a limit is reached. Data as a function of total ion source pressure and concentration were extrapolated by linear least squares to zero extraction voltage. The extrapolated values from all the data lead to the van't Hoff plot in Figure 4.

The data from Figure 4 result in a reaction enthalpy of −111 ± 2 kJ/mol (reported errors are one standard deviation) at the midtemperature of 576 K. Correcting the experimental data to 298 K using the computed geometry and vibrational frequencies results in an experimental association enthalpy of −115.0 kJ/mol at that temperature. The corrected experimental association enthalpy (Table 4) agrees well with the ab initio-predicted association enthalpy of −126 kJ/mol (Table 3). The computed S−S bond distance of 2.795 Å can be compared to an average S−S single-bond distance of about 2.05 Å.[65] The bond energy (about 40% of a normal 2c-2e S−S bond[66]), bond distance (about 135% of a normal 2c-2e S−S bond), and symmetric spin distribution between the two sulfur atoms all support the 2c-3e bonding picture. The geometry calculated at the MP2/6-31G(d) level (Figure 2) is in good agreement with the geometry reported earlier at the UHF/3-21G(d) level.[33]

(65) (a) For references to S−S bond lengths, see: Knop, O.; Boyd, R. J.; Choi, S. C. *J. Am. Chem. Soc.* **1988**, *110*, 7299. (b) Allen, F. H.; Kennard, O.; Watson, D. G.; Brammer, L.; Orpen, A. G.; Taylor, R. *J. Chem. Soc., Perkin Trans. 2* **1987**, S1.

(66) Chang, R. *Chemistry*, 4th ed.; McGraw-Hill, Inc.: New York, 1991; p 378.

Table 4. Experimental Heats of Formation and Association Enthalpies (kJ/mol) of 2c-3e Complexes[a]

	heats of formation (kJ/mol)		association enthalpy (kJ/mol)	
	$\Delta H^\circ_{f,0}$	$\Delta H^\circ_{f,298}$	$\Delta H^\circ_{rxn,0}$	$\Delta H^\circ_{rxn,298}$
$(SH_2)_2^+$ [b]	848.1	852.5	−119.6	−123.7
$(DMS)_2^+$	657.1	656.5	−115.6	−115.0
$(DES)_2^+$	533.4	532.3	−120.4	−119.3

[a] Based on experimental heats of formation of neutral and cation monomer,[37] experimental enthalpies of association, and theoretical heat capacity corrections. [b] G2 enthalpy of association is used.

The geometry of $[Me_2S\therefore SMe_2]^+$ (Figure 2) has C_{2h} symmetry. The tilt angle (the angle between the S−S bond and the line bisecting the C−S−C angle) is 95.6°. This is very similar to the calculated tilt angle in $[H_2S\therefore SH_2]^+$ (92.3°). The S∴S distance in $[Me_2S\therefore SMe_2]^+$ is shorter than in $[H_2S\therefore SH_2]^+$, possibly due to reduced electrostatic repulsion in $[Me_2S\therefore SMe_2]^+$ since there are more atoms to delocalize the positive charge.

The intercept of the van't Hoff plot (Figure 4) results in $\Delta S^\circ_{rxn,576} = -112 \pm 3$ J/mol K, while the predicted entropy of association is $\Delta S^\circ_{rxn,576} = -133$ J/mol K. These results are in excellent accord with that expected for an ion−molecule association reaction resulting in a strongly bound cluster.[67] The negative entropy change is mostly due to the loss of three translational degrees of freedom upon reaction. The experimental value for the entropy of reaction is just outside the range which was assumed (−84 to −105 J/mol K) in our previous estimate for this bonding interaction. The computational results for the $[Me_2S\therefore SMe_2]^+$ system are summarized in Table 3 at 298 K and 576 K (the midexperimental temperature) and in Table 4 where the experimental thermodynamic properties have been corrected to 0 and 298 K. The present experimental free energy of reaction at 525 K (−52.2 kJ/mol) differs somewhat from a previous determination at the same temperature (−56.1 kJ/mol) using a different ion source.[33] This ion source probably suffered from poor thermalization of all the ion source parts, especially the ion source exit slit which was probably colder than the ion source body, consistent with the direction of the difference between the two measurements.

$[Et_2S\therefore SEt_2]^+$. At low ionizing electron energies (near the threshold for formation of ions), three ions always present in the mass spectrum are Et_2S^+, $[Et_2S\therefore SEt_2]^+$, and $[Et_2S\therefore SEt]^+$, where the latter ion was less intense than the monomer and dimer ions but still present under all explored experimental conditions. However, we were unable to definatively determine if $[Et_2S\therefore SEt]^+$ originates from decomposition of the activated dimer complex or from electron impact fragmentation. Nevertheless we were able to establish equilibrium over a large temperature range (482−572 K). As the ionizing electron energy was increased, peaks which can be attributed to $[Et_2S\therefore SCH_2Et]^+$ and $[Et_2S_2]^+$ appeared in the mass spectrum. The ion intensity at *m/z* 165 due to $[C_7H_{17}S_2]^+$ increased with decreasing temperature, implying that $[C_7H_{17}S_2]^+$ results from a clustering reaction of *m/z* 75 $[C_3H_7S]^+$ with Et_2S.

The experimental equilibrium measurements on the $[Et_2S\therefore SEt_2]^+$ cluster were more challenging than those for $[Me_2S\therefore SMe_2]^+$. Under most conditions, RTD's showed that reaction 2 was close to equilibrium and started to merge as the extraction field was reduced (longer time). Figure 5 presents four distributions, two each for Et_2S^+ and $[Et_2S\therefore SEt_2]^+$ at different ion extraction fields. The figure clearly shows that the residence time distributions at shorter times are not identical but that the pair at the longer times are more similar. It was

(67) Keesee, R. G.; Castleman, A. W., Jr. *J. Phys. Chem. Ref. Data* **1986**, *15*, 1011.

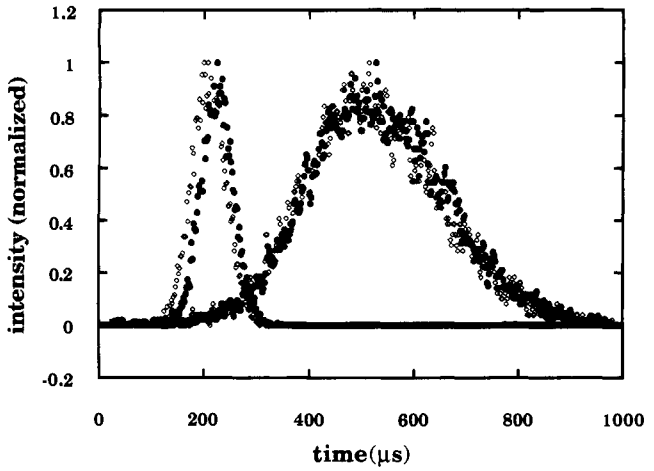

Figure 5. Residence time distributions for Et_2S^+ (open diamonds) and $[Et_2S\therefore SEt_2]^+$ (filled circles) at different ion extraction field strengths.

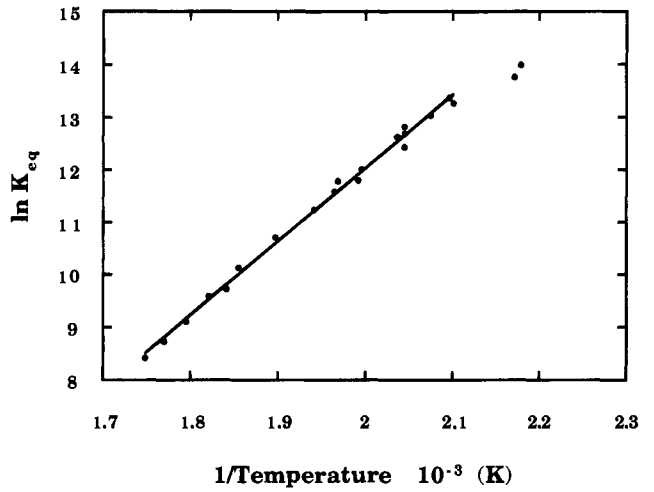

Figure 6. van't Hoff plot for reaction 2.

particularly difficult to reach equilibrium conditions at the lower temperatures. Much of our early data on reaction 2 did not fall on a linear van't Hoff line; rather it appeared that the data defined a limit for the line. As we gained experience with the chemical system, the van't Hoff plot in Figure 6 was collected. The data was obtained by extrapolating measured apparent equilibrium constants obtained as a function of ion extraction voltages to 0 V. Experiments at various total ion source pressures and composition were carried out. The two data points at the lowest temperatures in the van't Hoff plot shown in Figure 6 do not appear to fall on the line and were not included in the determination of the enthalpy and entropy of reaction. The least squares fit results in $\Delta H°_{rxn,520} = -116 \pm 2$ kJ/mol and $\Delta S°_{rxn,520} = -132 \pm 5$ J/mol K.

The monomers, SEt_2 and SEt_2^+, are much more flexible molecules than SMe_2 and SMe_2^+ and have multiple conformational minima. Three different structures were considered on the SEt_2 and SEt_2^+ potential energy surface. The lowest energy structures (**3a**,**a**$^+$) have C_{2v} symmetry and are in a trans−trans orientation with respect to rotation about the two S−C bonds (Figure 2). Two gauche−gauche structures were located; one pair were minima (**3b**,**b**$^+$) while the other pair were transition states (**3c**,**c**$^+$) at the HF/6-31G(d) level. Very close in energy to C_{2v} structures (**3a**,**a**$^+$) are the gauche−trans structures of C_1 symmetry (**3d**,**d**$^+$). At the PMP2/6-31G(d)+ZPC level, **3d** is only 0.2 kJ/mol higher in energy than **3a**, while **3d**$^+$ is 1.4 kJ/mol higher than **3a**$^+$. Entropy favors the lower symmetries of **3d**,**d**$^+$ over **3a**,**a**$^+$. As shown in Table 5, the free energy of **3d** is more favorable than that of **3a** by 1.5 kJ/mol at 298 K and by 2.7 kJ/mol at 520 K. The free energy of **3a**$^+$ is slightly lower than that of **3d**$^+$ but only by 1.2 kJ/mol at 520 K. Therefore, there exists the question about the appropriate reference monomers in calculating the binding energies. The free energy at 520 K favors the SEt_2 conformer **3d**, while it slightly favors the SEt_2^+ conformer **3a**$^+$. We have chosen to take **3a**,**a**$^+$ as the reference since they are the lowest energy conformers at 0 K.

Table 5. Calculated Relative Free Energies (kJ/mol) of DES and DES^+ Monomers[a]

	298 K		520 K	
sym	DES	DES^+	DES	DES^+
C_{2v} **3a**,**a**$^+$	0.0	0.0	0.0	0.0
C_2 **3b**,**b**$^+$	−0.1	5.4	−0.2	8.0
C_1 **3d**,**d**$^+$	−1.5	0.6	−2.7	1.2

[a] ΔG(rel to C_{2v}) = [ΔE(PMP2) + (0.9)ZPC + C_p(corr)] − $T\Delta S$.

The conformation surface of a related neutral molecule, divinyl sulfide, has been previously studied.[68] The two stable conformations, identified from a study of the potential energy surface at the HF/3-21G(d) level, could both be described as gauche−gauche conformations.[68a]

Two alternative 2c-3e complexes were considered for $[Et_2S\therefore SEt_2]^+$. The complexes most analogous to $[H_2S\therefore SH_2]^+$ and $[Me_2S\therefore SMe_2]^+$ is the $[Et_2S\therefore SEt_2]^+$ complex with C_{2h} symmetry. The $[Et_2S\therefore SEt_2]^+$ complex can be formed from $[Me_2S\therefore SMe_2]^+$ by replacing the hydrogen on Me_2S which points away from the opposite Me_2S with a methyl group. This replacement should give a structure which minimizes *intermoiety* steric repulsion in the complex between Et_2S, **3c**, and SEt_2^+, **3c**$^+$ but which may not minimize *intramoiety* repulsion (within each monomer unit in the $[Et_2S\therefore SEt_2]^+$ complex). This is particular evident as the **3c**,**c**$^+$ structures are 5.0 and 7.1 kJ/mol higher in energy than **3a**,**a**$^+$. A complex formed between **3a**,**a**$^+$ (not calculated) would have more intermoiety but less intramoiety repulsions. A compromise complex formed between **3d**,**d**$^+$ would have the advantage of having a very modest "cost" to adopt the higher energy conformer (**3d**,**d**$^+$ is 1.7 kJ/mol higher in energy than **3a**,**a**$^+$) yet not have unfavorable intermoiety repulsion. The complex between **3d**,**d**$^+$ has C_2 symmetry and is 7.0 kJ/mol lower in energy than the C_{2h} symmetry complex. Across the S∴S 2c-3e bond, two CH_2 groups are trans with respect to each other while the other two CH_2 groups are cis. The methyl groups are gauche−trans about the S-C bonds within each moiety, just as they are in **3d**,**d**$^+$.

The ab initio calculations at the PMP2/6-31G(d)//HF/6-31G(d) level predict a bond energy of 117.0 kJ/mol. At 298 K, $\Delta H°_{rxn}$ and $\Delta S°_{rxn}$ are −116 kJ/mol and −151 J/mol K, respectively. Correcting to 520 K, the thermodynamic values become −112 kJ/mol and −143 J/mol K which can be compared to the experimental values of −116 kJ/mol and −132 J/mol K, respectively. The predicted $[Et_2S\therefore SEt_2]^+$ geometry (Figure 2) has a S−S bond distance of 2.870 Å. Using the calculated molecular parameters to correct the experimental enthalpies to 0 K results in an experimental bond energy of 120.4 kJ/mol for $[Et_2S\therefore SEt_2]^+$ (Table 4).

Comparison of Calculated Properties of $[H_2S\therefore SH_2]^+$, $[Me_2S\therefore SMe_2]^+$, and $[Et_2S\therefore SEt_2]^+$. 1. Comparison of Monomer Ionization Energies. A comparison of adiabatic ionization energies is made with experiment in Table 6. As the level of theory improves, the difference between theory and experiment

(68) (a) Kimmelma, R.; Hotokka, M. *THEOCHEM* **1993**, *285*, 71. (b) Kao, J.; Eyermann, C.; Southwick, E.; Leister, D. *J. Am. Chem. Soc.* **1985**, *107*, 5323.

Table 6. Calculated Adiabatic Ionization Energies (eV)[a,b]

	IE/a	IE/b	IE/c
SH_2	9.82 (0.63)	10.18 (0.27)	10.43 (0.02)
DMS	8.24 (0.45)	8.52 (0.17)	
DES	7.99 (0.44)		

[a] Level a is PMP2/6-31G(d)//UHF/6-31G(d)+(0.9)ZPC. Level b is [PMP4/6-31+G(2df/p)]//UMP2/6-31G(d)+(0.9)ZPC. Level c is G2. [b] The values in parentheses are the difference between theory and experiment. The experimental values for SH_2, DMS, and DES are 10.45, 8.69, and 8.43 eV, respectively. Lias, S. G.; Bartmess, J. E.; Liebman, J. F.; Holmes, J. L.; Levin, R. D.; Mallard, W. G. *J. Phys. Chem. Ref. Data* **1988**, *17* (Suppl. 1). A similar value for the IE of DMS (8.64 eV) has recently been reported; see: Nourbakhsh, S.; Norwood, K.; Yin, H.-M.; Liao, C.-L.; Ng, C. Y. *J. Chem. Phys.* **1991**, *95*, 5014.

Table 7. Calculated Vibrational Frequencies (cm^{-1}) at the UHF/6-31G(d) Level Due to the Association of Two Monomers[a]

mode	$(SH_2)_2^+$ (C_{2h})	$(DMS)_2^+$ (C_{2h})	$(DES)_2^+$ (C_2)
S∴S stre	232 (230) a_g	283 (274) a_g	202 a
S∴S rock	587 (527) a_g	194 (187) a_g	182 a
S∴S rock	441 (427) b_u	194 (188) b_u	184 b
S∴S rock	456 (416) a_u	176 (161) a_u	98 a
S∴S rock	533 (470) b_g	175 (164) b_g	91 b
S∴S tors	66 (75) a_u	29 (32) a_u	19 a

[a] Values given in parentheses are calculated at MP2/6-31G(d).

Table 8. Calculated λ_{max} (transitions in nm) for Various 2c-3e Bonded Species[a]

	//UHF/6-31G(d)	//UMP2/6-31G(d)	exptl[b]
$(SH_2)_2^+ \cdot 4H_2O$	368	351	370
$(SH_2)_2^+$	405	396	370
$(DMS)_2^+$	476	452	465
$(DES)_2^+$	509		485

[a] Excitation energies were calculated with single excitations (CIS/6-31G(d)). [b] The experimental λ_{max} are measured in aqueous solution.[25]

decreases. The difference in the ionization energy of SH_2 between G2 and experiment is only 0.02 eV.

2. Comparison of New Frequencies. The new frequencies associated with the relative motions of the two sulfides in the 2c-3e complex are reported at the UHF/6-31G(d) level in Table 7 (MP2/6-31G(d) for $[H_2S\therefore SH_2]^+$ and $[Me_2S\therefore SMe_2]^+$). As one proceeds from $[H_2S\therefore SH_2]^+$ to $[Me_2S\therefore SMe_2]^+$ to $[Et_2S\therefore SEt_2]^+$, one finds the frequencies of associations (HF/6-31G(d)) to become smaller which simply reflects the increased reduced mass of the sulfide. The S∴S stretch remains relatively constant at about 200−280 cm^{-1}. In contrast, the torsional mode decreases from 66 to 29 to 19 cm^{-1} as one proceeds from $[H_2S\therefore SH_2]^+$ to $[Me_2S\therefore SMe_2]^+$ to $[Et_2S\therefore SEt_2]^+$. Since this mode is present in the product but not in reactants, entropy and heat capacity calculations will be very dependent on how accurately this mode is calculated. For example, an overestimation of the 19 cm^{-1} mode by only 10 cm^{-1}, would reduce the contribution by approximately 6.2 J/mol K at 298 K.

3. Comparison of λ_{max}. Since the magnitude of the splitting between the σ and σ^* orbitals is related to the degree of interaction between the two moieties forming the 2c-3e bond, λ_{max} is sometimes taken as an indicator of 2c-3e bond strength. On the basis of a series of measurements in aqueous solution, Asmus found[9-21,25] that the λ_{max} varied in a manner which could be related to the Taft σ^* value.[25] The values of λ_{max} for $[H_2S\therefore SH_2]^+$, $[Me_2S\therefore SMe_2]^+$, and $[Et_2S\therefore SEt_2]^+$ increase in the order 370, 465, and 485 nm which would indicate decreasing 2c-3e bond strength in that order (Table 8).

However, Clark[30] and Bally[26] have pointed out that alkyl substituents produce a red shift "independent of the steric interactions". The λ_{max} transition occurs from an orbital that has strong σ lone pair (perpendicular to S∴S axis) character to an orbital that has mostly p lone pair (parallel to S∴S axis) character. Alkyl substituents have the right symmetry to destabilize the σ lone pair orbital more than the p lone pair orbital resulting in a smaller energy gap and a red shift.

In order to explore the relationship between the optical transition and S∴S bond energies, we carried out theoretical calculations of the low-lying transitions. An electron correlation method of including single excitations was used[58] with the 6-31G(d) basis set (CIS/6-31G(d)) to determine the lowest three states. In each case, the lowest transition corresponded to an excitation from the doubly occupied lone pair combination orbital to the singly occupied sulfur−sulfur σ^* orbital.[26] Thus, the excitation was a $^2B_u \rightarrow {}^2Ag$ except for $[Et_2S\therefore SEt_2]^+$ which was a $^2B \rightarrow {}^2A$. The experimental trend of the first transition energy is reproduced (red shift) even though the S∴S bond strength remained essentially constant, varying less than 10 kJ/mol for the series.

Since λ_{max} was measured in aqueous solution, we were also interested in estimating the effect of solvation on λ_{max}, especially given the fact that the S∴S distance is predicted to decrease upon solvation (see above). In order to investigate this possibility, we calculated the lowest excitation energy for the $[(SH_2)_2]^+ \cdot 4H_2O$ complex. As discussed above, the four waters shorten the S∴S bond which results in a decrease of the wavelength needed for excitation (larger transition energy) by 37 nm at the CIS/6-31G(d)//UHF/6-31G(d) level and 45 nm at the CIS/6-31G(d)//MP2/6-31G(d) level. We conclude that solvation effects should cause a λ_{max} blue shift and that substituents which destabilize the σ lone pair in the 2c-3e complex should cause a red shift. We caution that extrapolation of λ_{max} trends to S∴S bond strength trends should be made with care since a blue shift (solvent induced) and a red shift (substituent induced) can occur without significantly affecting the S∴S bond strength.

4. Comparison of a_H Hyperfine Coupling Constants. Another point of contact between experiment and theory for 2c-3e bonded S∴S complexes is through a_H hyperfine coupling constants which have been reported for hydrogen in $[Me_2S\therefore SMe_2]^+$ and $[Et_2S\therefore SEt_2]^+$ complexes.[69-86] While the majority of unpaired spin is located evenly between the two

(69) Champagne, M. H.; Mullins, M. W.; Colson, A.-O.; Sevilla, M. D. *J. Phys. Chem.* **1991**, *95*, 6487.
(70) Ambroż, H. B.; Przybytniak, G. K.; Wrońska, T. *Radiat. Phys. Chem.* **1991**, *37*, 479.
(71) Nelsen, S. F. *J. Chem. Soc., Perkin Trans. 2* **1988**, 1005.
(72) Bonazzola, L.; Michaut, J. P.; Roncin, J. *Can. J. Chem.* **1988**, *66*, 3050.
(73) Williams, F.; Qin, X.-Z. *Radiat. Phys. Chem.* **1988**, *32*, 299.
(74) Qin, X.-Z.; Meng, Q.-C.; Williams, F. *J. Am. Chem. Soc.* **1987**, *109*, 6778.
(75) Qin, X.-Z.; Williams, F. *J. Chem. Soc., Chem. Commun.* **1987**, 257.
(76) Bonazzola, L.; Michaut, J. P.; Roncin, J. *J. Chem. Phys.* **1985**, *83*, 2727.
(77) Glidewell, C. *J. Chem. Soc., Perkin Trans. 2* **1985**, 299.
(78) Rao, D. N. R.; Symons, M. C. R.; Wren, B. W. *J. Chem. Soc., Perkin Trans. 2* **1984**, 1681.
(79) Davies, M. J.; Gilbert, B. C.; Norman, R. O. C. *J. Chem. Soc., Perkin Trans. 2* **1984**, 503.
(80) Glidewell, C. *J. Chem. Soc., Perkin Trans. 2* **1984**, 407.
(81) Wang, J. T.; Williams, F. *J. Chem. Soc., Chem. Commun.* **1981**, 1184.
(82) Chow, Y. L.; Iwai, K. *J. Chem. Soc., Perkin Trans. 2* **1980**, 931.
(83) Gilbert, B. C.; Marriott, P. R. *J. Chem. Soc., Perkin Trans. 2* **1979**, 1425.
(84) Gara, W. B.; Giles, J. R. M.; Roberts, B. P. *J. Chem. Soc., Perkin Trans. 2* **1979**, 1444.
(85) Petersen, R. L.; Nelson, D. J.; Symons, M. C. R. *J. Chem. Soc., Perkin Trans. 2* **1978**, 225.
(86) Gilbert, B. C.; Hodgeman, D. K. C.; Norman, R. O. C. *J. Chem. Soc., Perkin Trans. 2* **1973**, 1748.

Table 9. Comparison of Calculated and Experimental a_H Hyperfine Coupling Constants (G)[a,b]

	UHF/6-31G(d)//a	UHF/6-31G(d)//b	UHF/6-31+G(2df,p)//b	exptl
SH_2^+ (2H)	−33.4	−33.4	−26.1	
$SH_2^+ \cdot 2H_2O$ (2H)	−30.8	−30.1	−25.8	
$(SH_2)_2^+$ (4H)	−25.1	−20.1	−17.1	
$(SH_2)_2^+ \cdot 4H_2O$ (4H)	−19.5	−19.0	−16.4	
DMS^+ (6H)	16.7	18.0	16.9	20.4 (6H)[c]
$(DMS)_2^+$ (12H)	6.6	6.4	6.0	6.6 (12H)[d]
DES^+ **3a**$^+$ (4H)	22.3			18−20 (2H)[e]
DES^+ **3b**$^+$ (2H)	10.1			18−20 (2H)[e]
DES^+ **3d**$^+$ (4H)	15.1			18−20 (2H)[e]
$(DES)_2^+$ C_{2h} (8H)	3.0			6.9 (8H)[c]
$(DES)_2^+$ C_2 (8H)	6.9			6.9 (8H)[d]

[a] Level a indicates geometry optimization at UHF/6-31G(d), and level b indicates geometry optimization at UMP2/6-31G(d). [b] The Fermi contact integral is averaged over the number of hydrogens indicated in parentheses and multiplied by 1600.[87,88] [c] Reference 74. [d] Reference 83. [e] Reference 78.

sulfurs, sufficient spin density exists on hydrogens to give rise to a detectable ESR spectrum. From a computational point of view, a_H can be calculated by averaging the Fermi contact integral over the appropriate number of symmetry-equivalent hydrogens and multiplying by the constant 1600.[87,88] These results are reported in Table 9 where the Fermi contact integral is calculated with the UHF spin density. It is known that much improved results can be obtained when the Fermi contact integral is calculated with the UMP2 spin density.[87,88] However, our intention is only to determine whether the qualitative trends can be reproduced by theory. The answer to this question is yes. The changes in the value of a_H between the monomer and the 2c-3e bonded complex are well reproduced. The effect of the medium on the calculated a_H values can be determined by comparing calculations on $[H_2S\therefore SH_2]^+$ with and without explicit waters. Using the 6-31+G(2df,p) basis set, the difference in calculated values of a_H is less than 1 G.

IV. Conclusions

Experimental gas-phase bond energies have been determined for the 2c-3e S∴S bond in $[Me_2S\therefore SMe_2]^+$ and $[Et_2S\therefore SEt_2]^+$. Chemical equilibrium was established over a temperature range of 533−626 K for reaction 1 and over a range of 482−572 K for reaction 2. From van't Hoff plots, a value of 111 kJ/mol was determined for the bond enthalpy of the S∴S bond in $[Me_2S\therefore SMe_2]^+$ while a value of 116 kJ/mol was determined for the same bond in $[Et_2S\therefore SEt_2]^+$. Ab initio calculations on the 2c-3e bonded complexes, $[H_2S\therefore SH_2]^+$, $[Me_2S\therefore SMe_2]^+$, and $[Et_2S\therefore SEt_2]^+$, are in good agreement with experiment. At the highest level of theory, the S∴S bond energies are 120 kJ/mol (G2), 126 kJ/mol ([PMP4/6-31+G(2df,p)]), and 117 kJ/mol (PMP2/6-31G(d)), respectively. These binding energies are in the middle range of ion−molecule cation association enthalpies which vary from less than 20 kJ/mol to more than 200 kJ/mol.[67]

From a combination of experimental and theoretical data, we have estimated the heats of formation of the three complexes at 298 K to be 852.5, 656.5, and 532.3 kJ/mol, respectively. Other calculated properties include adiabatic ionization energies (for neutral monomers), excitation energies, and hydrogen hyperfine coupling constants. The wavelength value of the excitation energy agrees with the experimental trend observed by Asmus in solution.

Three conformers of Et_2S and Et_2S^+ were identified computationally. The most stable $[Et_2S\therefore SEt_2]^+$ complex (C_2 symmetry) occurs from the association of C_1 conformers (gauche−trans) of Et_2S and Et_2S^+. This complex has the best compromise of minimum intermoiety steric repulsion while maintaining a near optimal geometry of the monomers.

Acknowledgment. A.I. is very grateful to the donors of the Petroleum Research Fund administered by the American Chemical Society and the Auburn University Chemistry Department for financial support. Computer time for this study was made available by the Alabama Supercomputer Network and the NSF-supported Pittsburgh Supercomputer Center. We thank G. P. Ford for helpful discussions on the SH_2/H_2O calculations and T. R. Webb for previewing the manuscript.

(87) Cramer, C. J. *J. Org. Chem.* **1991**, *56*, 5229.
(88) Cramer, C. J. *J. Am. Chem. Soc.* **1991**, *113*, 2439.